

### Conclusion

The determination of the polarization vectors seems to involve a number of experimental problems (see for example, Dolling & Woods, 1965; Brockhouse, 1964). The recent evaluation of the polarization vector of the ferroelectric soft mode in  $\text{KD}_2\text{PO}_4$  by Skalyo, Frayer & Shirane (1970) is of some interest in this connexion. It is not possible to foresee all the obstacles that may be encountered when the anomalous scattering technique as proposed in this paper is used for determining the polarization vectors. It may be necessary to use lower concentrations of the anomalously scattering isotope in the specimen. However, in view of the inherent directness of this method, it appears worth while pursuing this experimental approach.

The authors wish to thank Mr Rajaram Nityananda for the discussions they had with him.

### References

- BROCKHOUSE, B. N. (1964). *Phonons and Phonon Interactions*, pp. 221–275. New York: Benjamin.
- COCHRAN, W. (1968). *Neutron Inelastic Scattering*, Vol. I, pp. 275–280. Vienna: IAEA. SM-104/121.
- DOLLING, G. & WOODS, A. D. B. (1965). *Thermal Neutron Scattering*, pp. 193–249. London: Academic Press.
- MARADUDIN, A. A., MONTROLL, E. W. & WEISS, G. H. (1963). *Theory of Lattice Dynamics in the Harmonic Approximation*. New York: Academic Press.
- PETERSON, S. W. & SMITH, H. G. (1961). *Phys. Rev. Letters*, **6**, 7.
- PETERSON, S. W. & SMITH, H. G. (1962). *J. Phys. Soc. Japan*, **17**, 335.
- RAMASESHAN, S. (1966). *Curr. Sci.* **35**, 87.
- RAMASESHAN, S. & VISWANATHAN, K. S. (1970). *Acta Cryst.* **A26**, 364.
- SINGH, A. K. & RAMASESHAN, S. (1968). *Acta Cryst.* **B24**, 35.
- SKALYO, J. JR, FRAZER, B. C. & SHIRANE (1970). *Phys. Rev.* **B1**, 278.

*Acta Cryst.* (1971). **A27**, 341

## The Performances of Neutron Collimators

### I. Accurate Transmitted Intensity Evaluations for Neutron Collimator Systems

BY F. ROSSITTO

*CESNEF, Politecnico di Milano, Milan, Italy*

AND G. POLETTI

*Gruppo Struttura della Materia, CISE, Milan, Italy*

(Received 2 October 1970)

Limitations imposed by the geometry of Soller collimator systems on luminosity and resolution of neutron diffraction equipment are studied on the grounds of angular and spatial distribution of neutrons. Transmission functions for collimator systems of arbitrary complexity are derived. The influence of the mutual distances among the various components of the experimental set-up on the shape of transmission functions is given in evidence. Careful intensity measurements performed with well diversified arrangements of Soller collimators are in fair agreement with our theoretical results. The way to improve the performances of neutron diffraction equipment by a proper choice of all the geometrical parameters is shown.

#### 1. Introduction

The influence of collimator parameters (typically the angular divergence) on luminosity and resolution of single or multi-axis neutron spectrometers is usually derived on the basis of Sailor's hypothesis (Sailor, Foote, Landon & Wood, 1956; Caglioti, Paoletti & Ricci, 1958, 1960; Caglioti & Ricci, 1962; Popovici & Gelberg, 1966). Sailor *et al.* (1956) assume that collimator transmission functions can be conveniently described by a Gaussian function  $n(\varphi)$ , where  $\varphi$  is the angle between the projection of any individual neutron trajectory on a horizontal plane and the collimator centre line; the full width at half maximum of the

Gaussian distribution is the angular divergence of the collimator.

Nevertheless neutron sources and collimators are quite sizeable, so that a more correct approach should take into account the dependence of transmission functions not only on direction but also on position of any individual neutron. In this last way Szabó (1959) and Jones (1962) worked out relations on intensity and parameter optimization limited to a single (primary) collimator, and Carpenter (1963) discussed a more general approach to the problem, giving a graphical representation of collimator transmission functions.

In the following sections we derive general transmission functions for neutron collimator systems, taking



Fig. 2 shows how the function  $A_h(x, \bar{z}, \varphi)$  can be evaluated. A well defined range of  $x$  values ( $x_1, x_2$ ) on the source plane corresponds to any emission angle  $\varphi$ , for which emerging neutrons are transmitted by the collimators and cross the reference plane, so defining a range ( $x'_1, x'_2$ ) in which all the neutrons emitted at an angle  $\varphi$  from the collimator centre line and belonging to the transmitted density are present. The interval  $\Delta x = x_2 - x_1$  and the interval  $\Delta x' = x'_2 - x'_1$  depend only on the collimator geometry:  $\Delta x = \Delta x' = s - l |\varphi| = s(1 - |\varphi|/\alpha)$ . A plot of  $x$  as a function of  $\varphi$  at  $z = \bar{z}$  for all the allowed neutron trajectories is illustrated in Fig. 3.

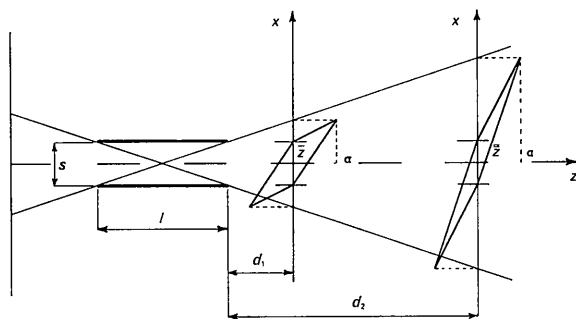


Fig. 4. Dependence of  $A_h$  on the distance from the outlet surface of the collimator.

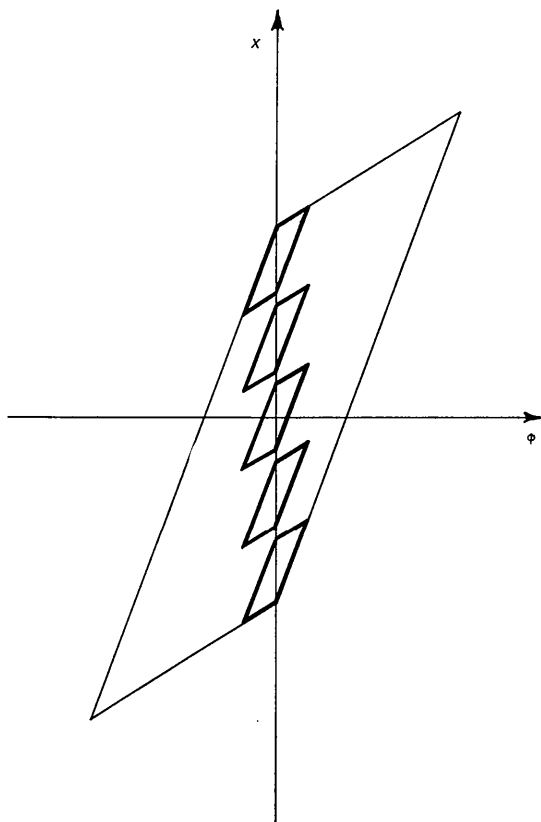


Fig. 5. 5-slit collimator transmission function representation in the horizontal plane (see text).

$A_h(x, \bar{z}, \varphi)$  is unity inside the parallelogram, and zero everywhere outside. The function  $A_v(y, \bar{z}, \psi)$  is similarly defined and exhibits the same properties. According to equation (1), and also, since the product

$$A_h(x, \bar{z}, \varphi) \cdot A_v(y, \bar{z}, \psi)$$

can take only 1 or 0 values, the function  $A(x, y, \bar{z}, \varphi, \psi)$  is the transmission function wanted for a rectangular single-slit collimator. Its analytical definition for a collimator of length  $l$ , width  $s$  and height  $h$ , located at a distance  $d$  from the reference plane, follows from the parallelogram edge equations:

$$\begin{aligned} \varphi \geq 0 \quad & \begin{cases} x_2 = d\varphi + s/2 \\ x_1 = (d+l)\varphi - s/2 \end{cases} & \varphi \leq 0 \quad & \begin{cases} x_2 = (d+l)\varphi + s/2 \\ x_1 = d\varphi - s/2 \end{cases} \\ \psi \geq 0 \quad & \begin{cases} y_2 = d\psi + h/2 \\ y_1 = (d+l)\psi - h/2 \end{cases} & \psi \leq 0 \quad & \begin{cases} y_2 = (d+l)\psi + h/2 \\ y_1 = d\psi - h/2 \end{cases} \end{aligned} \quad (2)$$

While the knowledge of density is of main importance when dealing with the interaction of neutrons with a monochromating crystal or a sample in the beam, the performances of collimator systems are more conveniently discussed in terms of intensity. The overall transmitted intensity, evaluated on the reference plane, is

$$I = \int_{-\infty}^{+\infty} \int_{-\infty}^{+\infty} \int_{-\infty}^{+\infty} \int_{-\infty}^{+\infty} S(x, y, 0, \varphi, \psi) \times A(x, y, \bar{z}, \varphi, \psi) dx dy d\varphi d\psi \quad (3)$$

In most cases of practical interest, the neutron source can be considered uniform and isotropic, so that its density is a constant  $C$  (neutrons/cm<sup>2</sup>.sterad.sec). Therefore

$$I = \int_{-\infty}^{+\infty} \int_{-\infty}^{+\infty} \int_{-\infty}^{+\infty} \int_{-\infty}^{+\infty} C \cdot A(x, y, \bar{z}, \varphi, \psi) dx dy d\varphi d\psi \quad (3.1)$$

and remembering equation (1).

$$\begin{aligned} I &= C \cdot \left( \int_{-\infty}^{+\infty} \int_{-\infty}^{+\infty} A_h(x, \bar{z}, \varphi) dx d\varphi \right) \\ &\quad \times \left( \int_{-\infty}^{+\infty} \int_{-\infty}^{+\infty} A_v(y, \bar{z}, \psi) dy d\psi \right) \\ &= C \cdot \mathbf{A}_h \cdot \mathbf{A}_v = C \cdot G_{(1)} \end{aligned} \quad (3.2)$$

where  $\mathbf{A}_h$  and  $\mathbf{A}_v$  are the parallelogram areas in the horizontal ( $x, \varphi$ ) plane and in the vertical ( $y, \psi$ ) plane, respectively. Integration limits suit the definition of the  $A$  functions. Equation (3.2) shows that the intensity evaluated on the reference plane is equal to the neutron density  $C$  of the source times the product of the areas of the two  $A$  parallelograms, which is a geometrical factor  $G_{(1)}$  directly proportional to the overall transmitted intensity. (The subscript (1) stands for a single-slit collimator.) Note that the parallelogram areas  $\mathbf{A}_h$  and  $\mathbf{A}_v$  [and therefore the value of the integral (3.2)] are clearly independent of  $\bar{z}$ , while it is shown in Fig. 4

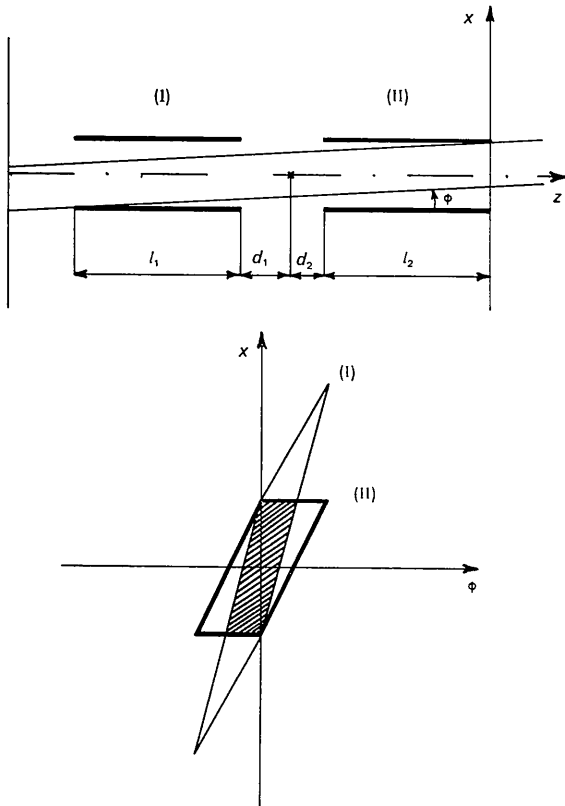


Fig. 6. Two-collimator system transmission function evaluated on a reference plane located at the outlet surface of the second collimator.

that the transmission functions are dependent on  $\bar{z}$  (and hence on  $d$ ). The geometrical factor  $G_{(1)}$  is no longer proportional to the overall transmitted intensity in the general case referred to in equation (3).

Extension of the above arguments and calculations to multi-slit Soller collimators is straightforward; in fact transmissions by each slit are independent of one another, and equation (1) is still valid, so we can separate the variables, as we did before. The  $A$  function is graphically represented in the horizontal plane by as many parallelograms as the collimator has slits, while in the vertical plane it consists of only one parallelogram. A typical situation in the horizontal plane is shown in Fig. 5, in which the shadow effect due to the separation shims is also displayed (the larger parallelogram represents the transmission function that would be obtained by removing the shims). Note that there is no overlap among the parallelograms (the slits do not interact with one another), the separation shims being perfect absorbers. Consequently the overall intensity transmitted by an  $n$ -slit Soller collimator is given by

$$I = \sum_{i=1}^n \int_{-\infty}^{+\infty} \int_{-\infty}^{+\infty} \int_{-\infty}^{+\infty} \int_{-\infty}^{+\infty} S(x, y, 0, \varphi, \psi) \times A_i(x, y, \bar{z}, \varphi, \psi) dx dy d\varphi d\psi \quad (4)$$

where  $A_i$  is the transmission function of the  $i$ th slit. If the density of the neutron source equals the constant  $C$ , equation (4) can be rewritten:

$$I = C \cdot A_h \cdot A_v = C \cdot G_{(n)} \quad (5)$$

where  $A_h$  is the sum of the parallelogram areas in the horizontal plane, and  $A_v$  is the area of the parallelogram in the vertical plane;  $G_{(n)}$  then represents the geometrical factor, directly proportional to the overall transmitted intensity, for an  $n$ -slit Soller collimator.

(b) A collimator system in the beam

Collimator systems can be dealt with in a very simple way, thanks to the above described properties of the  $A$  functions. In fact, in the absence of scattering, the transmission events through each collimator of the system are independent; for example the overall transmission function  $A_{12}(x, y, \bar{z}, \varphi, \psi)$  for a two in-line collimator system is the product of the transmission functions  $A_1$  and  $A_2$  of the two collimators. Remembering equation (1)

$$A_{12}(x, y, \bar{z}, \varphi, \psi) = A_{h1}(x, \bar{z}, \varphi) \cdot A_{h2}(x, \bar{z}, \varphi) \cdot A_{v1}(y, \bar{z}, \psi) \cdot A_{v2}(y, \bar{z}, \psi) \quad (6)$$

where the  $A$  functions will be in general of the type shown in Fig. 5. This means that the transmission event can be described in two planes normal to each

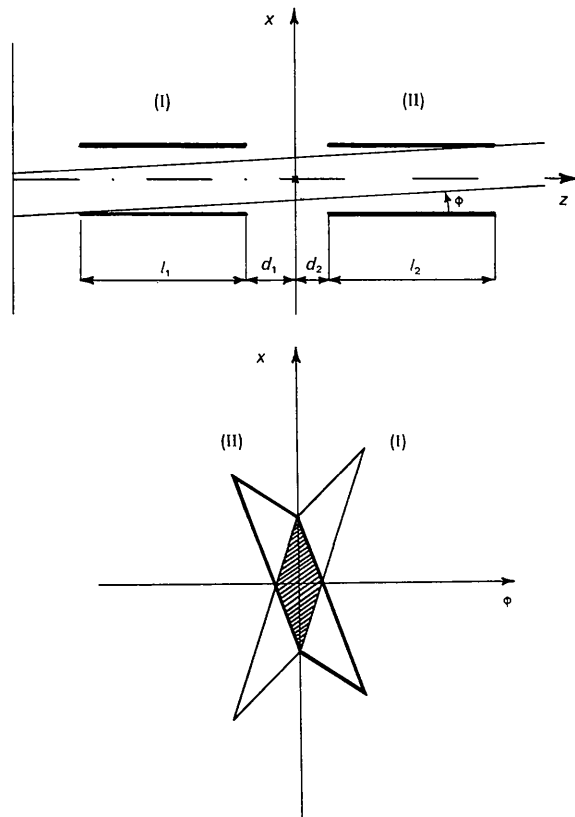


Fig. 7. Two-collimator system transmission function evaluated on a reference plane passing through the rotation axis.

other, considering in each plane one collimator at a time, as in § 2(a). The graphical representation of the  $A_{12}$  function then consists of two sets of overlapping parallelograms, whose common parts are regions in which  $A_{12}$  is unity. This is shown in Fig. 6, which refers to the transmission in the  $(x, \phi)$  plane of a system of two single-slit collimators. To deal with particular problems (e.g. the direct beam curve interpretation) it is often more convenient to refer intensity calculations to a suitable plane, namely that passing through a rotation axis of the diffraction equipment. This is also allowed by the properties of the transmission functions  $A$ . The result is shown in Fig. 7. Note that the two shadowed areas in Figs. 6 and 7 are equal.

The neutron intensity transmitted by a two collimator system is given by

$$I = \int_{-\infty}^{+\infty} \int_{-\infty}^{+\infty} \int_{-\infty}^{+\infty} \int_{-\infty}^{+\infty} S(x, y, 0, \phi, \psi) \times A_{12}(x, y, \bar{z}, \phi, \psi) dx dy d\phi d\psi \quad (7)$$

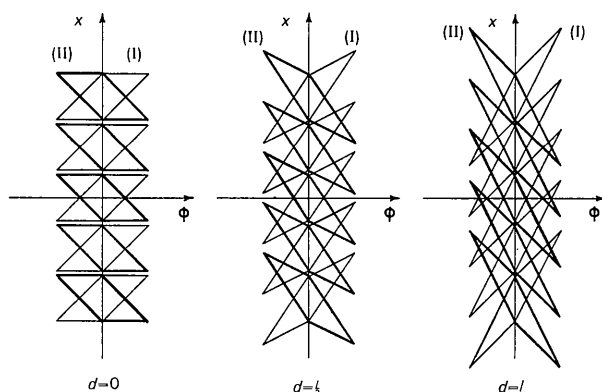


Fig. 8. Dependence of two identical 5-slit collimator system transmission function on the distance  $d$  from the rotation axis. The higher order overlaps are shown; from left to right  $k=0, k=1, k=2$ .

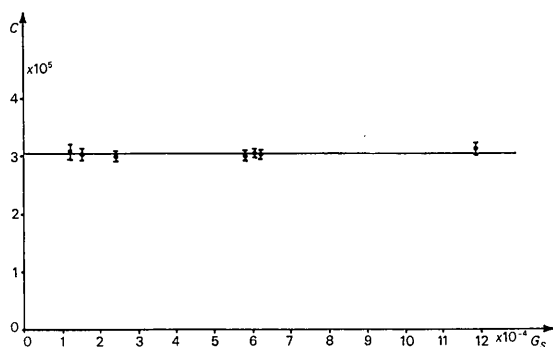


Fig. 9. Neutron source density  $C$  as evaluated for different collimator arrangements. Note that the  $G_s$  values are relative to differences both in arrangements and in the features of the collimating elements. The mean value per unit power level of the reactor (full line) is  $C = 3.045 \times 10^5 \pm 1.7\%$  neutrons/cm<sup>2</sup>.sterad. sec.W.

and when the neutron source density is constant, we can write

$$I = C \cdot G_S \quad (8)$$

where the geometrical factor  $G_S$  is

$$G_S = \int_{-\infty}^{+\infty} \int_{-\infty}^{+\infty} \int_{-\infty}^{+\infty} \int_{-\infty}^{+\infty} A_{12}(x, y, \bar{z}, \phi, \psi) dx dy d\phi d\psi = \left( \int_{-\infty}^{+\infty} \int_{-\infty}^{+\infty} A_{h1}(x, \bar{z}, \phi) A_{h2}(x, \bar{z}, \phi) dx d\phi \right) \times \left( \int_{-\infty}^{+\infty} \int_{-\infty}^{+\infty} A_{v1}(y, \bar{z}, \psi) A_{v2}(y, \bar{z}, \psi) dy d\psi \right). \quad (9)$$

In this case the factor  $G_S$  (as  $G_{(1)}$  and  $G_{(n)}$ ) is directly proportional to the overall transmitted intensity.

Neutrons transmitted by one slit of the first Soller collimator in the system may pass through several slits of the second collimator; consequently the parallelograms involved in the graphical representation overlap, giving rise to new contributions to the transmitted intensity, as shown in Fig. 8. This will be discussed in § 4.

Calculations of  $G_S$  by means of equation (9) may become very complicated in general; nevertheless this trouble may be overcome by graphical evaluation of the areas of the overlapped parallelograms, on the basis of their edge equations.

### 3. Experiments and discussion

Neutron transmitted intensities have been measured by means of a standard single-axis crystal spectrometer [an improved version of that described by Giacchetti, Musci & Poletti (1963)], whose first collimator was located inside a radial beam-hole of the L-54M reactor operating at C.E.S.N.E.F. Geometrical parameters of the collimator system (overall length and width of collimators, number and thickness of the shims, angular divergence of each collimating element of Sollers) could be varied in a wide range; the distance of collimators from spectrometer rotation axis could be changed too. All the used collimators were of black-wall type, since the surface of the shims were coated with myristic acid, which is effective to suppress neutron total reflexion (Jones & Bartolini, 1963; Rossitto & Terrani, 1967). Neutrons were detected by means of a cylindrical BF<sub>3</sub> proportional counter, located along the axis of the second collimator, whose surface was large enough to collect all the neutrons transmitted by the collimator system.

To optimize the geometry of diffraction equipment and to check the effectiveness of the outlined approach, careful measurements of neutron intensity transmitted by a system consisting of two black-wall Soller collimators in line have been performed in different experimental arrangements. The values of the collimator parameters  $s_{tot}$ ,  $h$  and  $l$  were held constant, while those of the number  $n$  of slits and then of the

angular divergence  $\alpha$  of each slit were varied in a wide range. In this way arrangements both usual and quite unusual in neutron diffraction experiments were tested to ensure generality of conclusions. From experimental data concerning the intensity transmitted by different collimator systems, the source neutron density has been drawn by means of equation (8) and the results are shown in Fig. 9. Equation (8) requires that the neutron source is uniform and isotropic, as is often found. The evaluation of the geometrical factors  $G_S$  has been carried out in general on the lines sketched in § 2(b). Only in some particularly significant cases analytical relations for  $G_S$  have been derived, as will be shown in § 4. The agreement among the values obtained for the source density in the various examined arrangements of collimators is quite satisfactory and shows that the rôle played by the various parameters involved has been properly described.

Our experimental results point out that the hypothesis on the source nature is quite reasonable. The result enables one to establish the source neutron density (if constant) with great accuracy, employing a very simple collimation system, even consisting of single-slit collimators. Once the source density is known, the calculation of neutron intensity transmitted by a collimation system, however complicated, is an easy job [equation (8)], since the factor  $G_S$  explicitly includes the dependence of the transmitted intensity on all the geometrical parameters of the equipment considered. A further check of the theory will be given in a later paper, in which neutron intensities transmitted by systems of two Soller collimators are discussed as a function of the angle between the collimator centre lines. Experimental data are compared with theoretical results obtained with the use of the approach previously outlined: the agreement is quite good over the whole of the angular range explored.

#### 4. Two-collimator system: dependence of the transmitted intensity on the mutual distance

We now derive relations, useful to choose the best values for geometrical parameters of a neutron diffraction experimental set-up. To simplify calculations we discuss the behaviour of a system of two identical Soller collimators located at equal distances from the rotation axis. This can be done with no loss in generality. Let us study the behaviour of the neutron intensity transmitted by such a system as a function of the distance of the collimators from the rotation axis, when the number  $n$  of the slits is changed. Again we suppose the length  $l$ , the height  $h$  and the total width  $s_{\text{tot}}$  of the collimators are fixed. The contribution of a single slit of the system to the geometrical factor  $G_S$  is

$$A_0 = \frac{s^2 h^2}{4(d+l)^2} = \frac{sh\alpha\beta}{4(1+d/l)^2} \quad (10)$$

where  $\alpha = s/l$  and  $\beta = h/l$  are the angular divergences in the horizontal and vertical plane respectively, and  $s =$

$[s_{\text{tot}} - (n-1)v]/n$ , where  $v$  is the thickness of the shims. Therefore the geometrical factor for  $n$  slits, in the absence of overlaps, is

$$G_0 = nA_0 \quad (11)$$

and when  $k$  overlaps occur [as mentioned in § 2(b)]

$$G_S = G_0 + G_1 + \dots + G_k \\ = nA_0 + (n-1)A_1 + \dots + (n-k)A_k \quad (12)$$

where

$$A_k = \frac{\left[ \left( 2\frac{d}{l} - \frac{v}{s} \right) - (k-1) \left( 1 + \frac{v}{s} \right) \right]^2}{2\frac{d}{l} \left( 1 + \frac{d}{l} \right) \left( 1 + 2\frac{d}{l} \right)} \\ \times \frac{s^2 h^2}{2l^2 \left( 1 + \frac{d}{l} \right)} \quad (k \geq 1). \quad (13)$$

Now putting  $x = d/l$  and  $\gamma = v/s$

$$A_k = \frac{[(2x - \gamma) - (k-1)(1 + \gamma)]^2}{x(1 + 2x)} \times \frac{sh\alpha\beta}{4(1+x)^2} \quad (14)$$

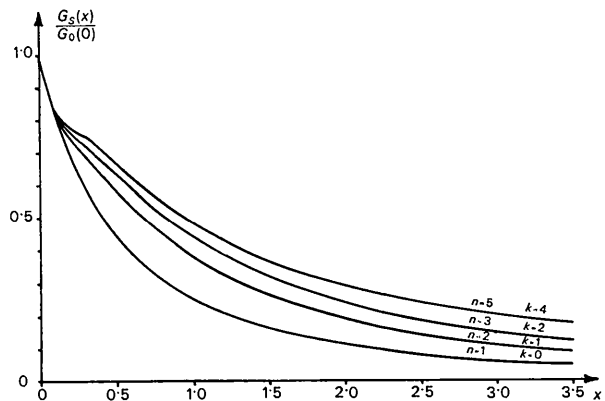


Fig. 10. Dependence on  $x = d/l$  of the geometrical factor  $G_S$  for  $n = 1, 2, 3, 5$  and  $k = 0, 1, 2, 4$  respectively.

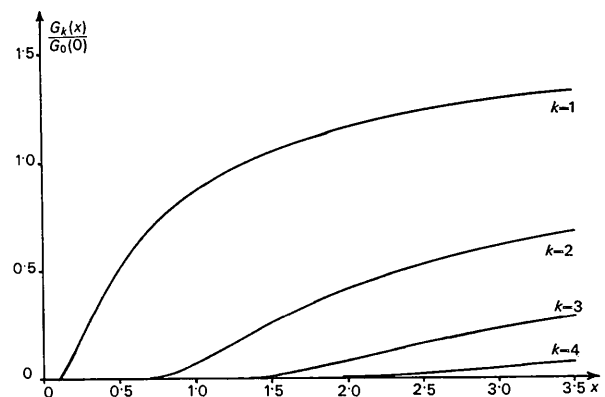


Fig. 11. Relative weight of higher order overlaps for a  $n = 5$  two an collimator system as a function of  $x = d/l$ .

and

$$G_S(x) = \frac{nsh\alpha\beta}{4(1+x)^2} + \sum_{j=1}^k (n-j) A_j(x). \quad (15)$$

The  $j$ th overlap occurs at that value of  $x=x(j)$  for which the numerator in equation (14) vanishes, so that

$$x(j) = \frac{j(1+\gamma)-1}{2}. \quad (16)$$

The geometrical factor for collimators joined together ( $x=0$ ) and therefore with no overlap is given by equation (11) which can be rewritten

$$G_0(0) = \frac{nsh\alpha\beta}{4}. \quad (17)$$

The dependence of  $G_S$  on the mutual distances between the collimators can be put in better evidence introducing equation (17) in equations (14) and (15) and studying the ratio  $G_S(x)/G_0(0)$  that is independent of  $s$ ,  $h$ ,  $\alpha$  and  $\beta$

$$\frac{G_S(x)}{G_0(0)} = \frac{1}{(1+x)^2} + \sum_{j=1}^k \frac{n-j}{n} \times \frac{[(2x-\gamma)-(j-1)(1+\gamma)]^2}{\times(1+2x)(1+x)^2}. \quad (18)$$

Fig. 10 shows a plot of  $G_S(x)/G_0(0)$  as a function of  $x$  for several different values of the slit number  $n$ . The intensity enhancements due to the overlap effects at the various  $x(j)$  are clearly shown. Fig. 11 is a plot of  $G_k(x)/G_0(x)$  as a function of  $x$  for a system made up of two Soller collimators with  $n=5$  slits. It represents the contribution of each  $k$ th overlap to the total transmitted intensity (in units of transmitted intensity without overlap) as a function of  $x$ . It can be easily realized that  $G_k(x)$  can reach very high values for  $k=1$  [in the range of 100 to 200% over the values of  $G_0(x)$ ].

As to the dependence of the neutron intensity transmitted by a collimator system on the horizontal angular divergence  $\alpha$  of the Soller slits, it is easy to derive the following relations from equations (10) and (13).

$$G_0(x) = \frac{nh^2\alpha^2}{4(1+x)^2} \quad (19)$$

$$A_k(x) = \frac{[(2x-\gamma)-(k-1)(1+\gamma)]^2}{4x(1+2x)} \times \frac{h^2\alpha^2}{(1+x)^2}. \quad (20)$$

Therefore the geometrical factor  $G_S(x)$  is proportional to  $\alpha^2$  and so is the transmitted intensity. Nevertheless, owing to the influence of the other geometrical parameters on the intensity equations (10) and (13), this result can undergo immediate experimental check only for a system in which  $n$ ,  $h$ ,  $v$  and the ratio  $d/l$  are kept constant.

## 5. Conclusions

The results we have obtained above for systems of two identical Soller collimators are valid for more complicated systems, as to the dependence of the transmitted intensity on the more significant parameters of the experimental arrangements. Analytical calculations may be troublesome, but graphical evaluations can be performed quickly and easily in any case, as indicated in § 2(b).

Therefore, from a quite general point of view, it is evident that correct and complete insight into the investigated phenomena can be reached by taking into account the spatial neutron distribution in addition to the angular one.

## References

- CAGLIOTI, G., PAOLETTI, A. & RICCI, F. P. (1958). *Nucl. Instrum.* **3**, 223.  
 PAOLETTI, A. & RICCI, F. P. (1960). *Nucl. Instrum. Methods*, **9**, 195.  
 CAGLIOTI, G. & RICCI, F. P. (1962). *Nucl. Instrum. Methods*, **15**, 155.  
 CARPENTER, J. M. (1963). TID-18397.  
 GIACCHETTI, G., MUSCI, M. & POLETTI, G. (1963). *Energia Nucleare*, **10**, 173.  
 JONES, I. R. (1962). *Rev. Sci. Instrum.* **33**, 1399.  
 JONES, I. R. & BARTOLINI, W. (1963). *Rev. Sci. Instrum.* **34**, 28.  
 POPOVICI, M. & GELBERG, D. (1966). *Nucl. Instrum. Methods*, **40**, 77.  
 ROSSITTO, F. & TERRANI, M. (1967). *Nucl. Instrum. Methods*, **55**, 288.  
 SAILOR, V. L., FOOTE, H. L. JR, LANDON, H. H. & WOOD R. E. (1956). *Rev. Sci. Instrum.* **27**, 26.  
 SZABÓ, P. (1959). *Nucl. Instrum. Methods*, **5**, 184.